

The Status of Saturation, CGC and Glasma

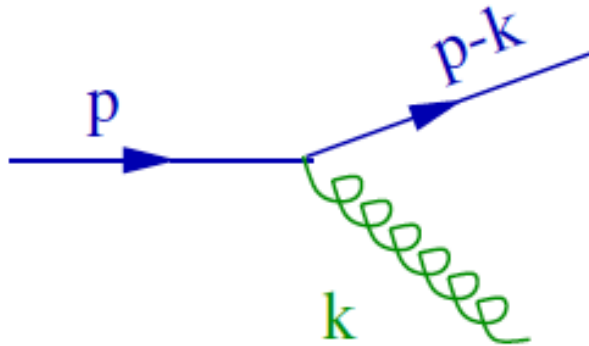
« What have we learned from RHIC? »

BNL, May 12, 2010

Summary - Orsay 8/06/10

J.-P. Blaizot, IPhT, CEA Saclay and CNRS

Radiation and multiplication of partons



$$d\mathcal{P} \simeq \alpha_s \frac{dk_{\perp}^2}{k_{\perp}^2} \frac{dx}{x}$$

One can calculate the change of the wave-function (its ‘**evolution**’), **not** the wave-function itself -> **Evolution equations** (with respect to directions of enhanced emission):

$$\frac{dk_{\perp}^2}{k_{\perp}^2} \longrightarrow d \ln Q^2$$

DGLAP

$$\frac{dx}{x} \longrightarrow d \ln \frac{1}{x}$$

BFKL

Growth of structure functions is tamed by
non-linear evolution

[Gribov, Levin, Ryskin,83']

For instance,

$$\frac{\partial^2 xG(x, Q^2)}{\partial \ln(1/x) \partial \ln Q^2} = \frac{3\alpha_s}{\pi} xG(x, Q^2) - \frac{3\alpha_s^2}{\pi^2 R^2} \frac{[xG(x, Q^2)]}{Q^2}$$

[Gribov, Levin, Ryskin,83' - Mueller, Qiu, 86']

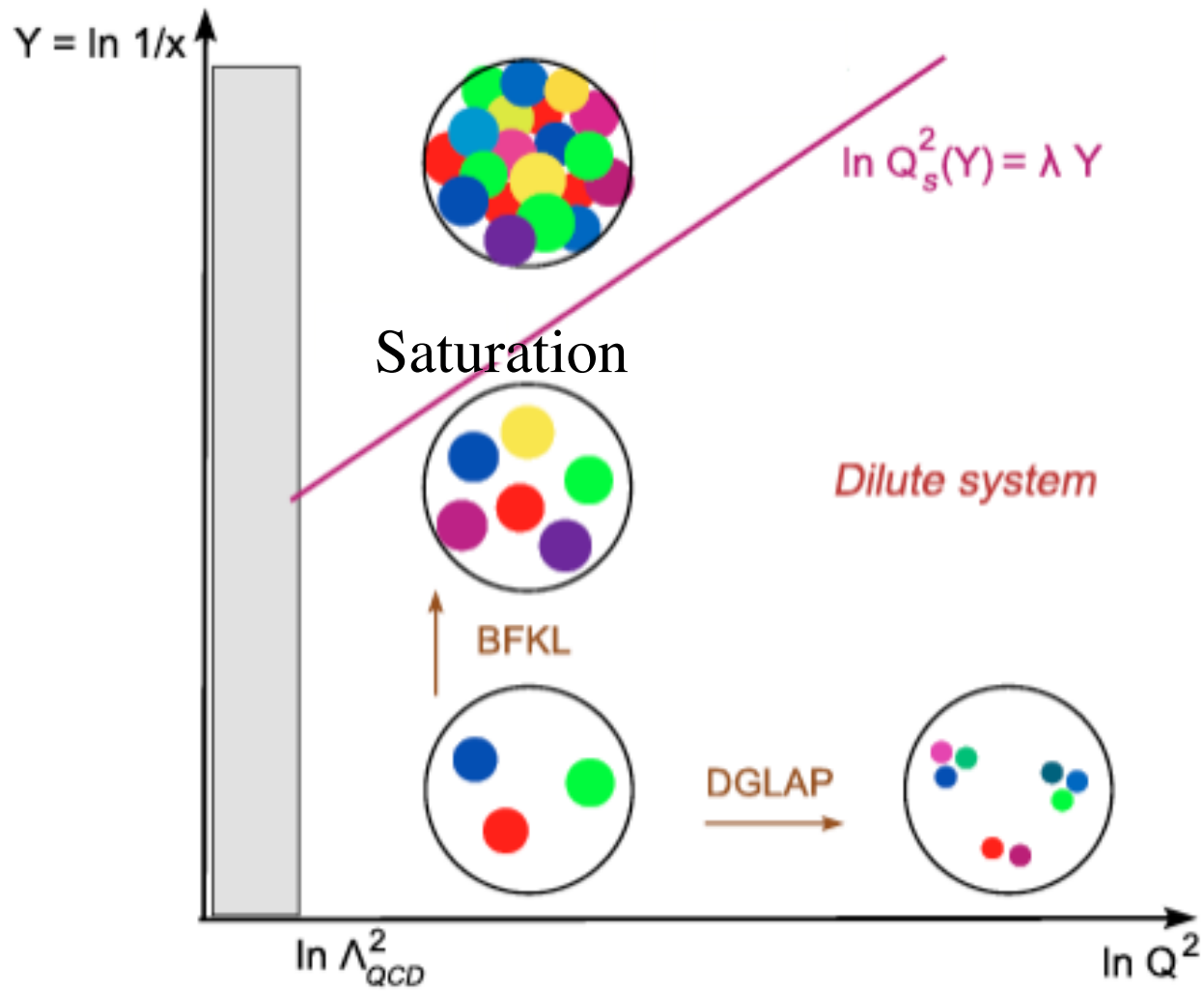
Emergence of a scale: the saturation momentum

$$Q_s^2 = \frac{\alpha_s}{\pi R^2} xG(x, Q_s^2)$$

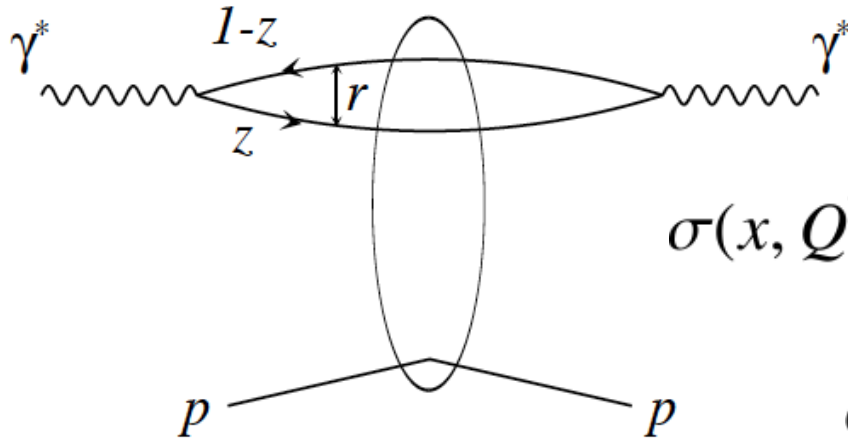
More elaborate equations have been derived (BK, JIMWLK, ..)

(More on these soon !)

The qualitative picture



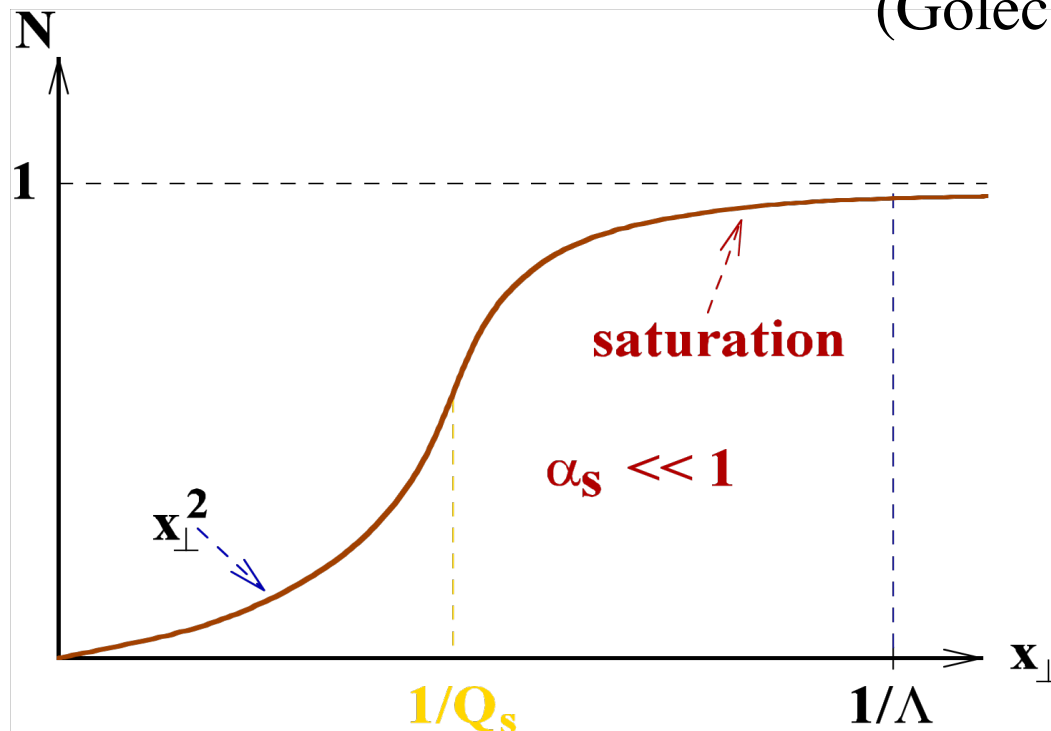
Seeing saturation in DIS



$$\sigma(x, Q^2) = \int d^2\mathbf{r} \int dz |\psi(z, \mathbf{r})|^2 \hat{\sigma}(x, r^2)$$

$$\hat{\sigma}(x, r^2) = \sigma_0 \left(1 - e^{-r^2 Q_s^2/4}\right)$$

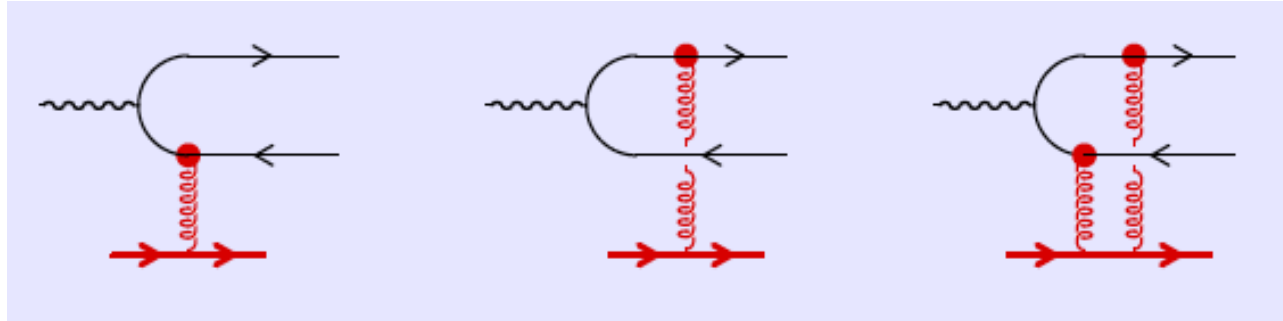
(Golec-Biernat, Wüsthoff, 98')



(from Kovchegov)

CGC and Glasma

Focus on small x (or rapidity) evolution



$$\sigma_{dipole} = \frac{2}{N_c} \int d^2 x_{\perp} \text{Tr} \left\langle 1 - U \left(x_{\perp} + \frac{r_{\perp}}{2} \right) U^{\dagger} \left(x_{\perp} - \frac{r_{\perp}}{2} \right) \right\rangle_Y$$

$$U(x_{\perp}) = P \exp \left\{ ig \int dx^{-} A^{+}(x^{-}, x_{\perp}) \right\}$$

$$\langle \cdots \rangle_Y = \int \mathcal{D}A |\Phi_Y[A]|^2 \langle A | \cdots | A \rangle$$

During interaction process, the field A of the target is frozen
(separation of scales - adiabatic approximation)

'Classical CGC'

McLerran Venugopalan Model

$$\left[D_\mu, F^{\mu\nu} \right] = J^\nu \quad (\text{frozen source})$$

$$J^\mu = \delta^{\mu+} \rho(x_\perp, x^-)$$

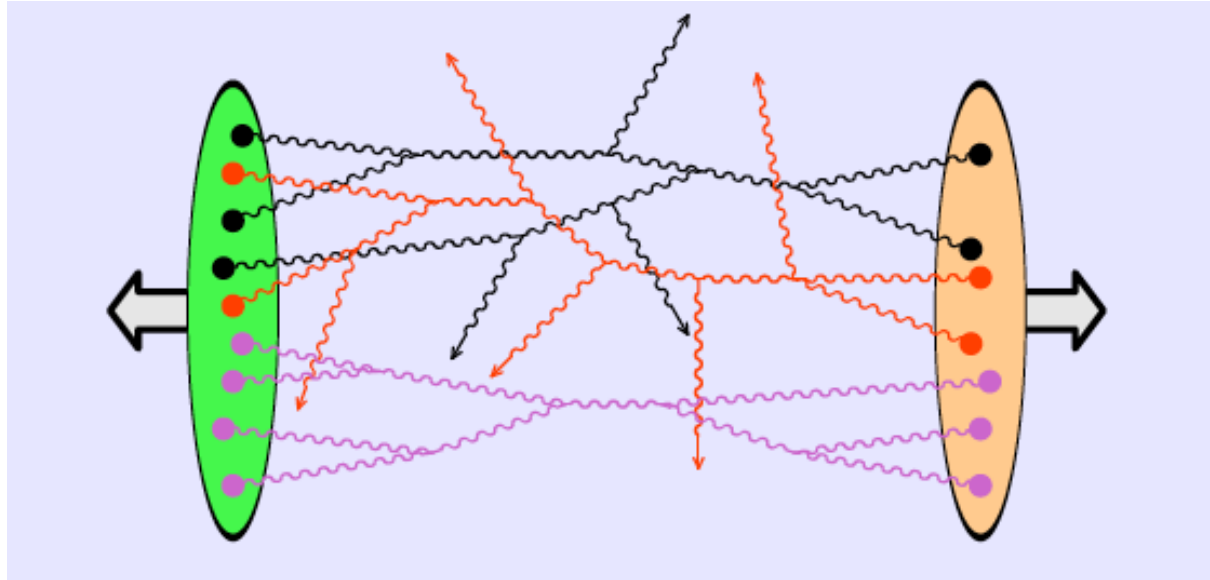
Gaussian average over color source

$$\langle \rho^a(x_\perp, x^-) \rho^b(y_\perp, y^-) \rangle = g^2 \mu \delta^{ab} \delta(x_\perp - y_\perp) \delta(x^- - y^-)$$

Capture some features of saturation $Q_s^2 \sim g^2 \mu$

But no evolution. Often used as 'initial condition'.

From the wave function to the initial stage of nucleus-nucleus collisions : the Glasma



(Gelis)

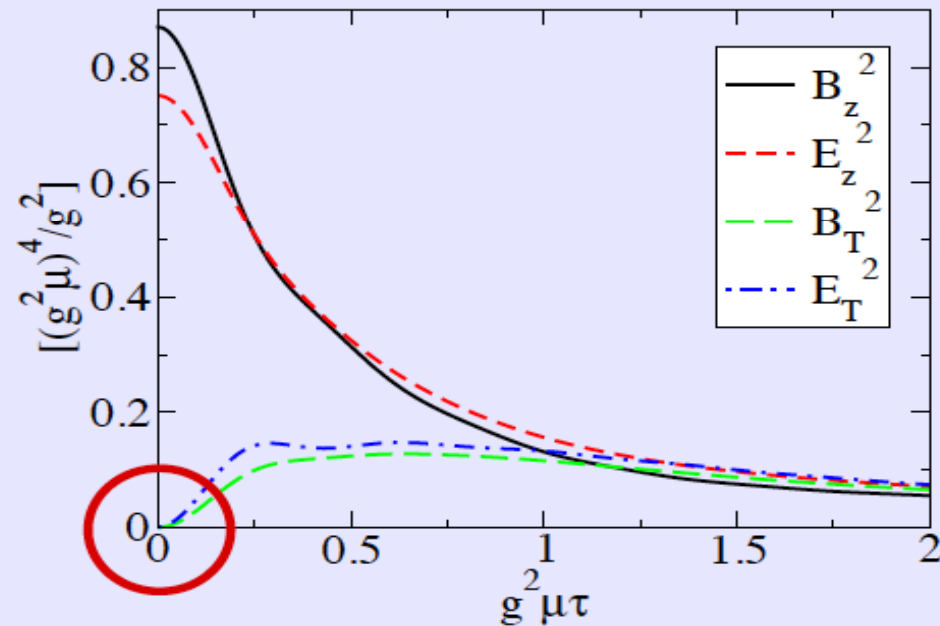
Energy-Momentum tensor at Leading Log accuracy

$$\langle T^{\mu\nu}(\tau, \eta, \vec{\mathbf{x}}_{\perp}) \rangle_{\text{LLog}} = \int [D\rho_1 D\rho_2] W_1[\rho_1] W_2[\rho_2] \underbrace{T_{\text{LO}}^{\mu\nu}(\tau, \vec{\mathbf{x}}_{\perp})}_{\text{for fixed } \rho_{1,2}}$$

Initial classical fields, Glasma

Lappi, McLerran (2006)

- Immediately after the collision, the chromo- \vec{E} and \vec{B} fields are purely longitudinal and boost invariant :



- **Glasma** = intermediate stage between the CGC and the quark-gluon plasma

Phenomenology

CGC calculations and
'CGC inspired' models
confronted to data

$$Q_s^2 = Q_0^2 \left(\frac{x_0}{x} \right)^\lambda \quad Q_0^2 \propto A^{1/3} \quad Q_s^2(b) = Q_s^2(0) \sqrt{1 - b^2/R^2}$$

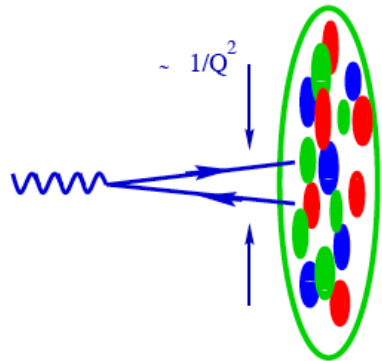
$$\alpha_s = \alpha_s(Q_s)$$

$$\frac{dN}{dy d^2 p_T} \sim \frac{1}{p_T^2} \int \frac{d^2 k_T}{(2\pi)^2} \phi_A(x_1, k_T) \phi_B(x_2, p_T - k_T)$$

DEEP INELASTIC SCATTERING (Diffraction)

Geometrical scaling

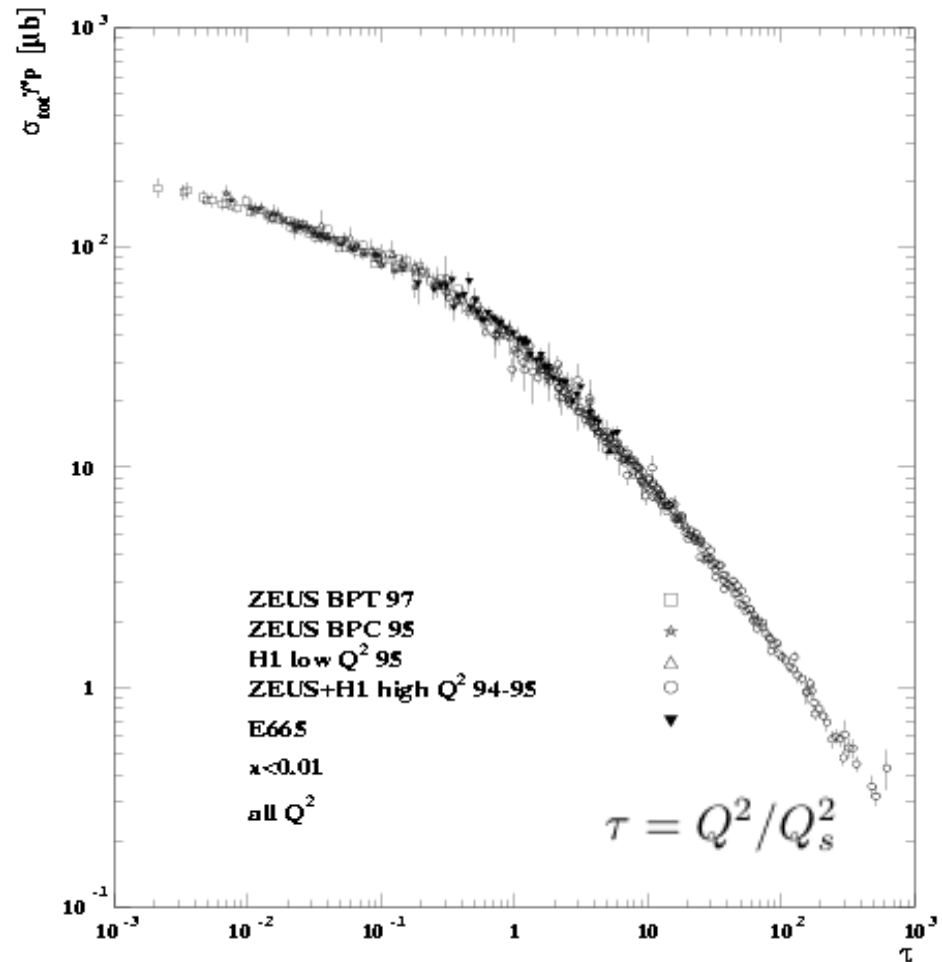
$$\sigma_{\gamma^*A}(x, Q^2) = \int dz \int d^2\mathbf{r} \underbrace{|\psi(z, \mathbf{r}; Q^2)|^2}_{QED} \underbrace{2 \int d^2\mathbf{b} (1 - S_\tau(\mathbf{x}, \mathbf{y}))}_{\sigma_{dipole}}$$



$$\sigma_{dip} = \sigma_0 [1 - \exp(-r_\perp^2 Q_s^2(x))]^2$$

$$Q_s^2(x) \equiv Q_0^2 \left(\frac{x_0}{x}\right)^\lambda$$

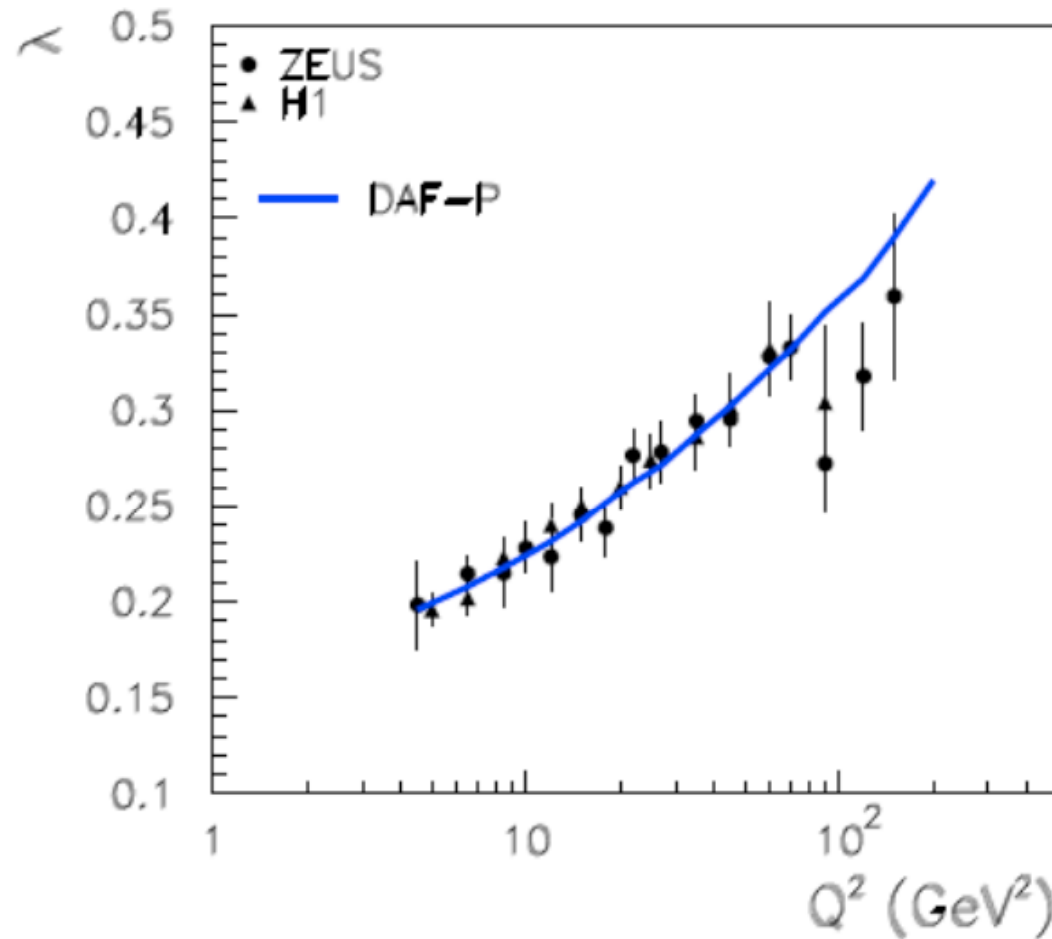
(Golec-Biernat, Kwiecinski, Stasto)



(H. Kowalski)

The rate of rise λ

$$F_2 \sim (1/x)^\lambda$$



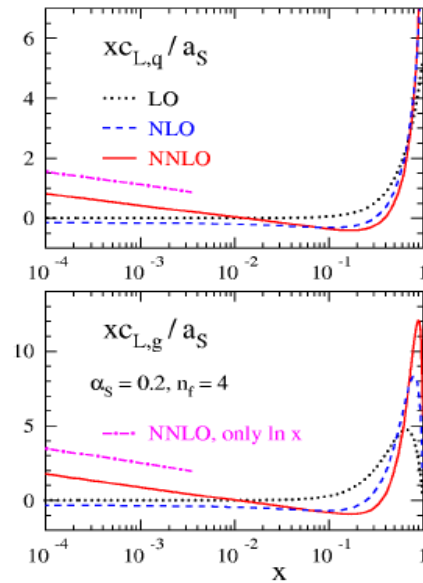
The first successful pure BFKL description of the λ plot.

For many years it was claimed that BFKL analysis was not applicable to HERA data because of the observed substantial variation of λ with Q^2

SMALL x PHYSICS FROM THE PERTURBATIVE END THE NNLO CORRECTIONS

THEORY

THE COEFFICIENT FUNCTION C_L
(Moch, Vermaseren, Vogt 2005)

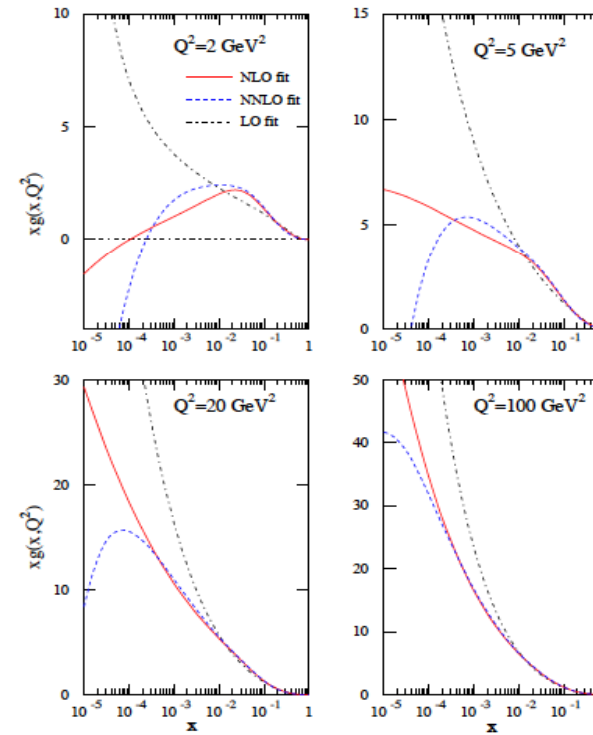


- PERTURBATION THEORY UNSTABLE
- LEADING LOG APPROX POOR

PHENOMENOLOGY

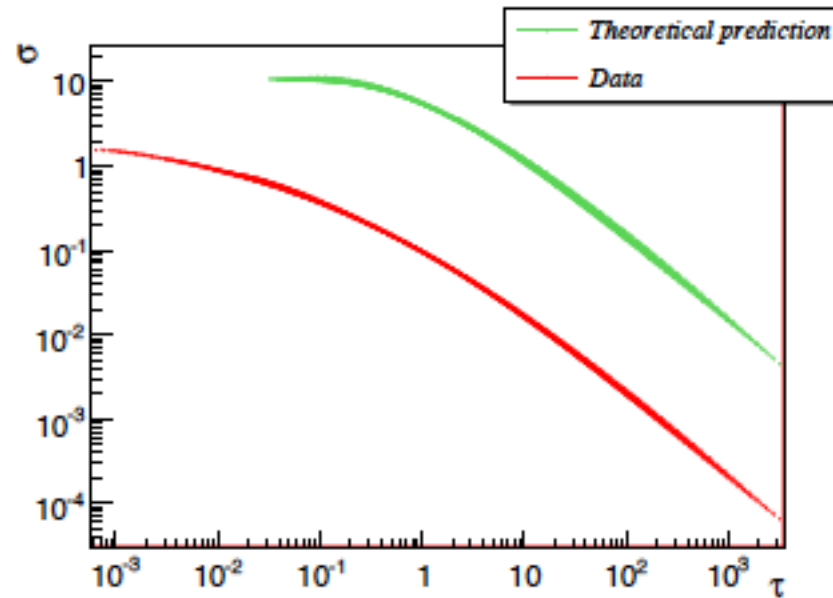
THE BEST-FIT GLUON

(Moch, Vermaseren, Vogt 2005)



(S. Forte)

Geometric scaling from DGLAP



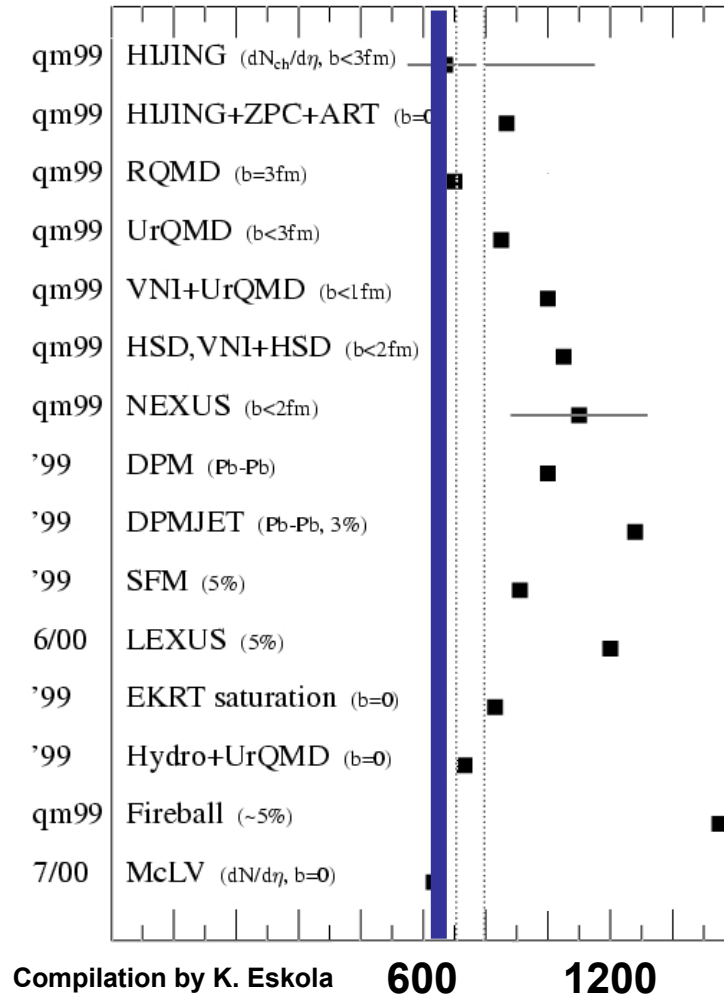
From F. Caola, in arXiv 0901.2504

Nucleus-nucleus collisions
Proton-nucleus collision

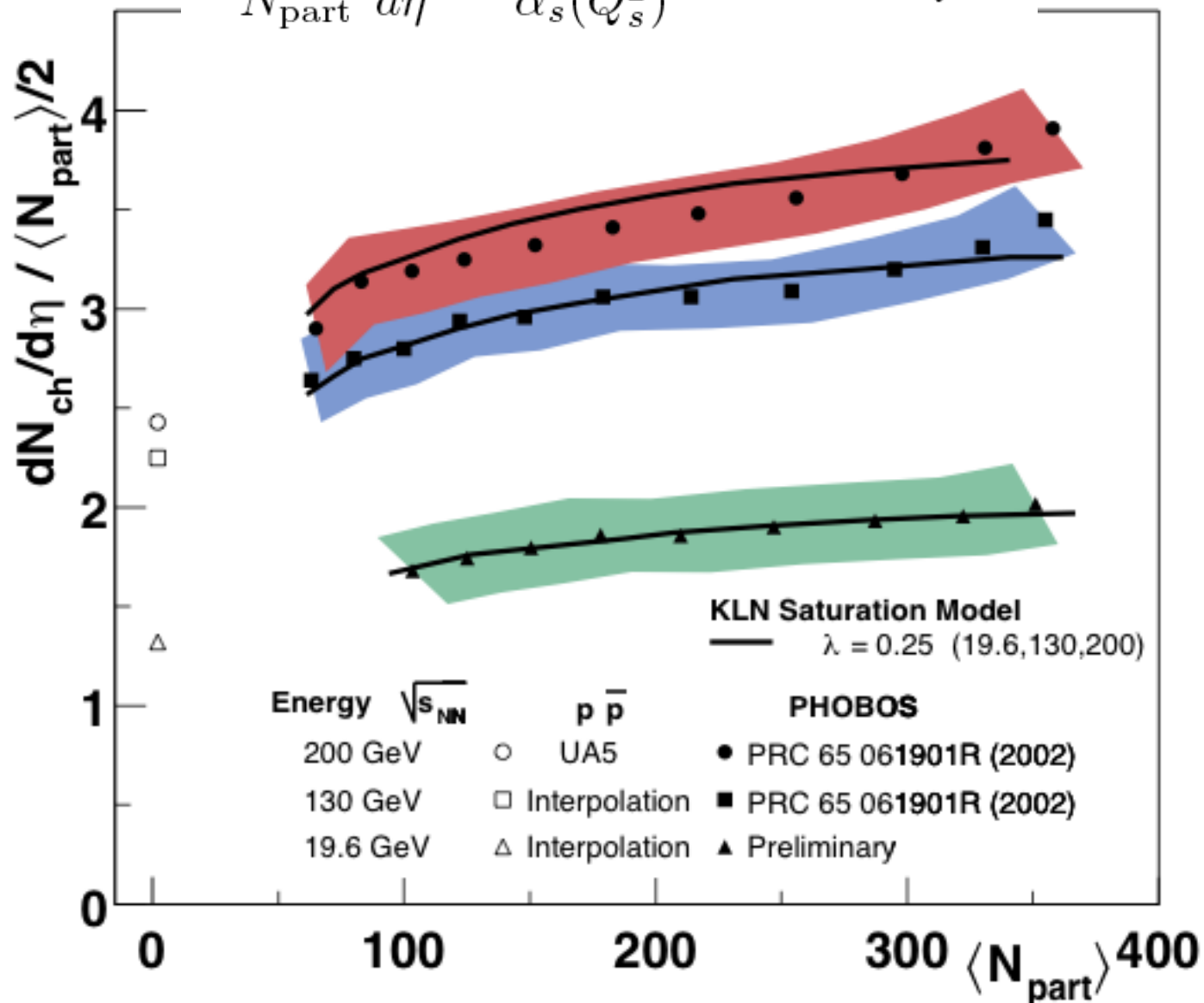
Particle multiplicities

Total multiplicities

PHOBOS Central Au+Au (200 GeV)



$$\frac{1}{N_{\text{part}}} \frac{dN}{d\eta} \sim \frac{1}{\alpha_s(Q_s^2)} \sim \ln(Q_s^2/\Lambda_{QCD}^2)$$

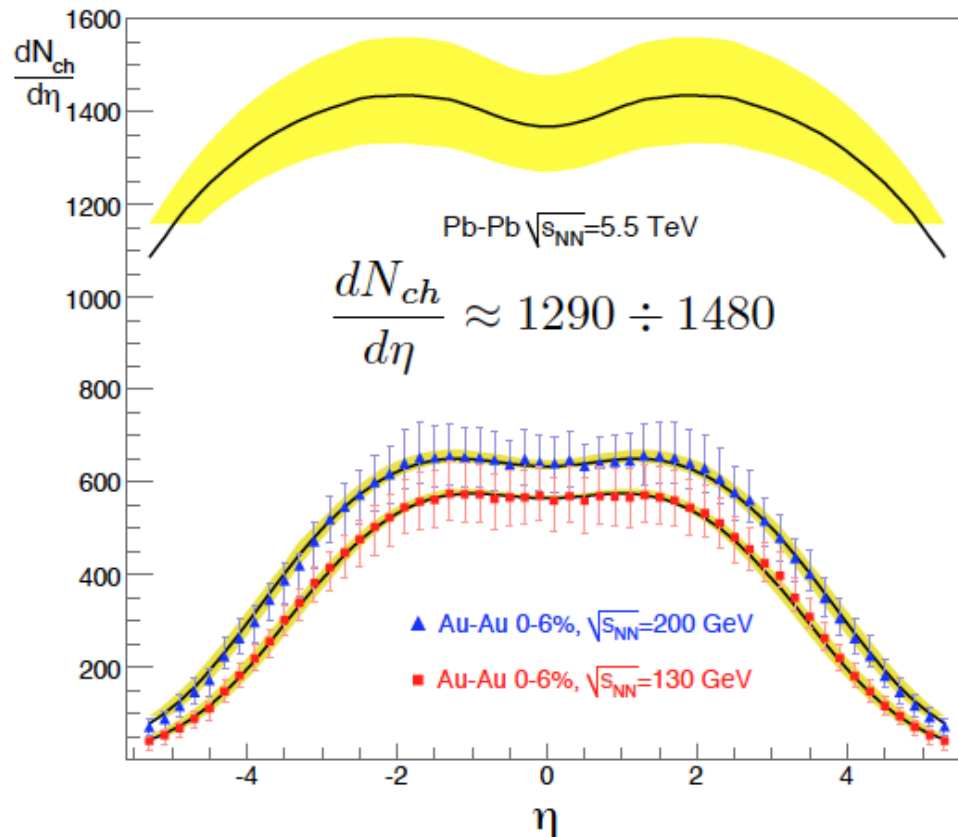


(Albacete)

Fit parameters consistent with NLO-CGC analyses of other observables:

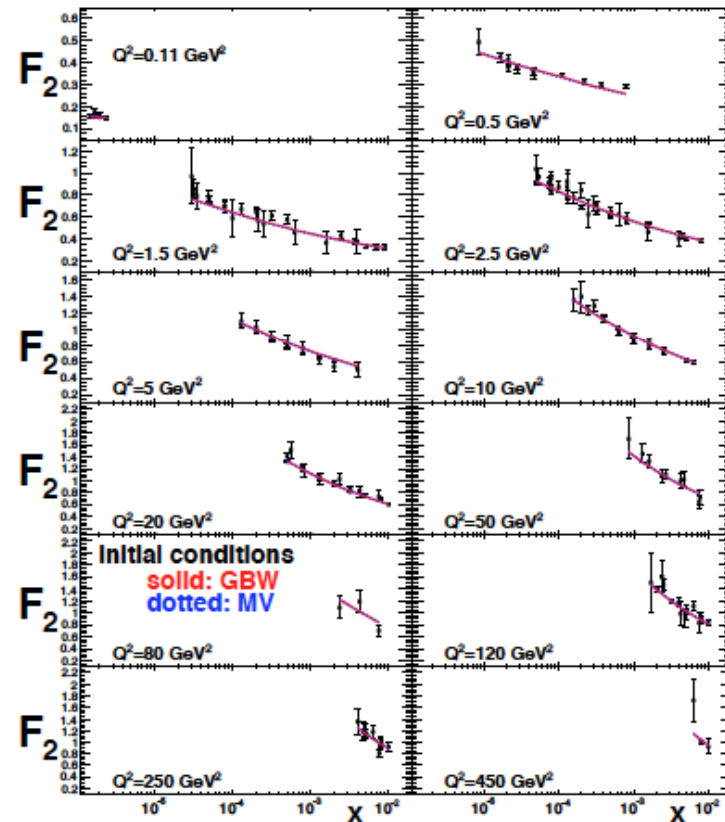
Multiplicities in RHIC Au+Au

JLA



F_2 , F_L and F_D in e+p HERA collisions

JLA-Armesto-Milhano-Salgado
Goncalves et al.



$$\frac{Q_{0A}^2}{Q_{0proton}^2} \sim 2 \div 2.5 = cA^{1/3} \quad \text{compatible with e+A data. K. Dusling et al}$$

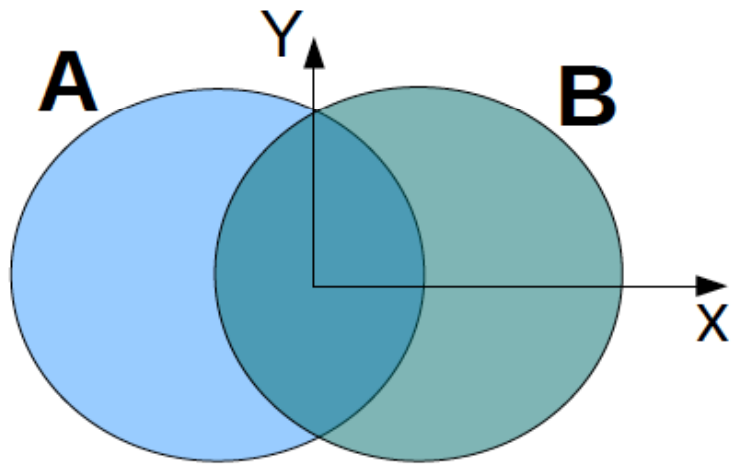
Two-particle correlations in forward d+Au at RHIC (Cyrille Marquet's talk)

Transverse density:

(Dumitru)

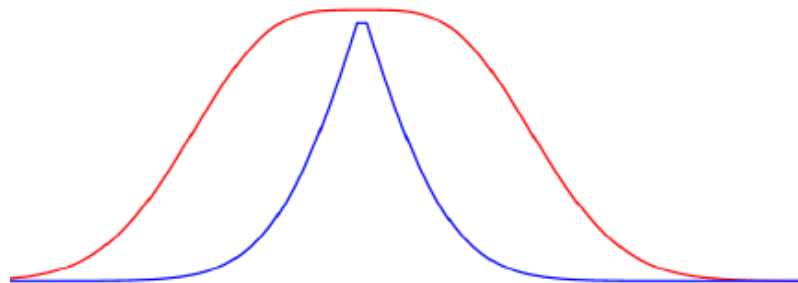
nucl-th/0605012

$$\frac{dN_g}{d^2 r_\perp dy} = \frac{\Upsilon \pi N_c}{N_c^2 - 1} \int \frac{d^2 p_t}{p_t^2} \int d^2 k_t \alpha_s \phi(x_\perp, k_t^\perp) \phi(x_\perp, (p_t - k_t)^\perp)$$
$$\sim \underline{\underline{Q_{s\ min}^2}} \log \frac{Q_{s\ max}^2}{Q_{s\ min}^2}$$



$$\text{CGC: } \frac{dN}{dy d^2 r} \sim \min(\rho_{\text{part}}^A, \rho_{\text{part}}^B)$$

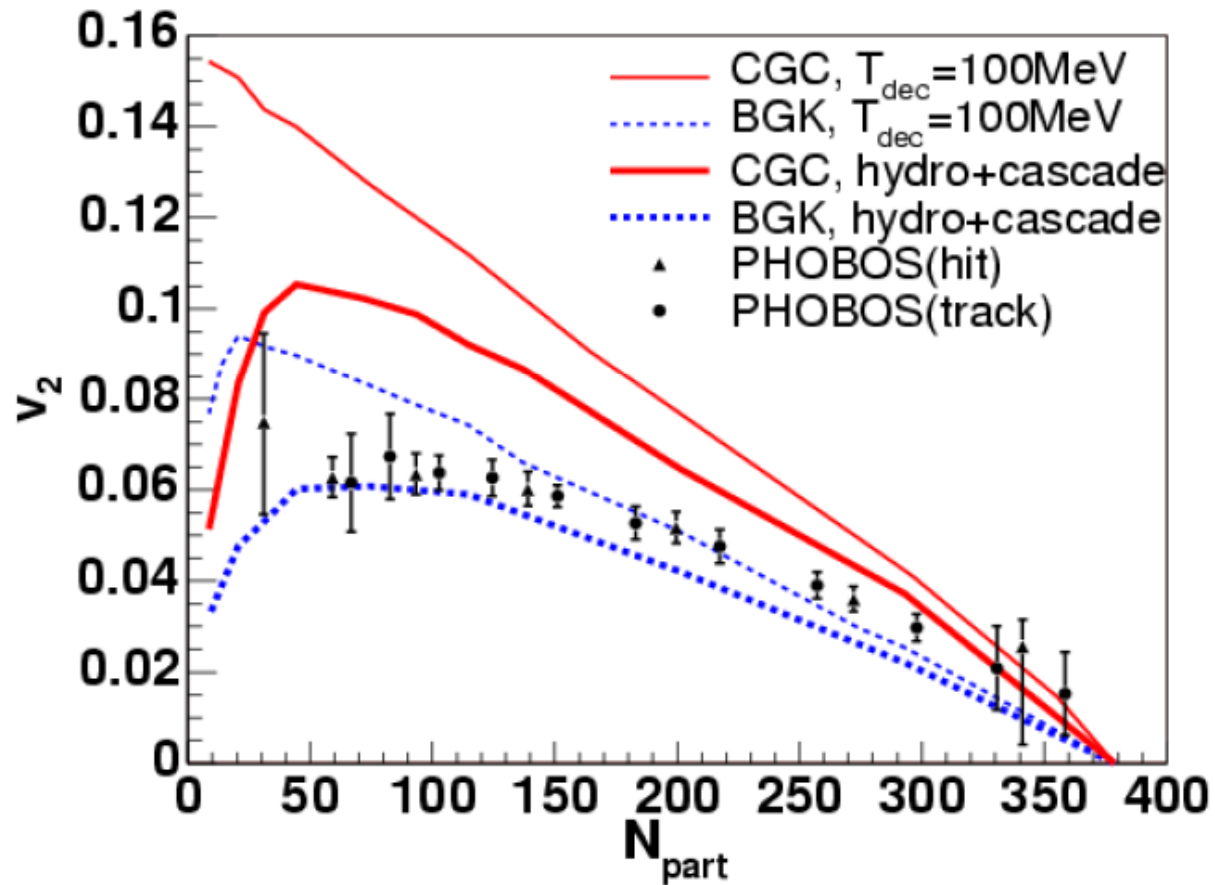
$$\text{Glauber: } \frac{dN}{dy d^2 r} \sim \frac{\rho_{\text{part}}^A + \rho_{\text{part}}^B}{2}$$



$$\epsilon_{\text{CGC}} > \epsilon_{\text{Glauber}}$$

(Dumitru)

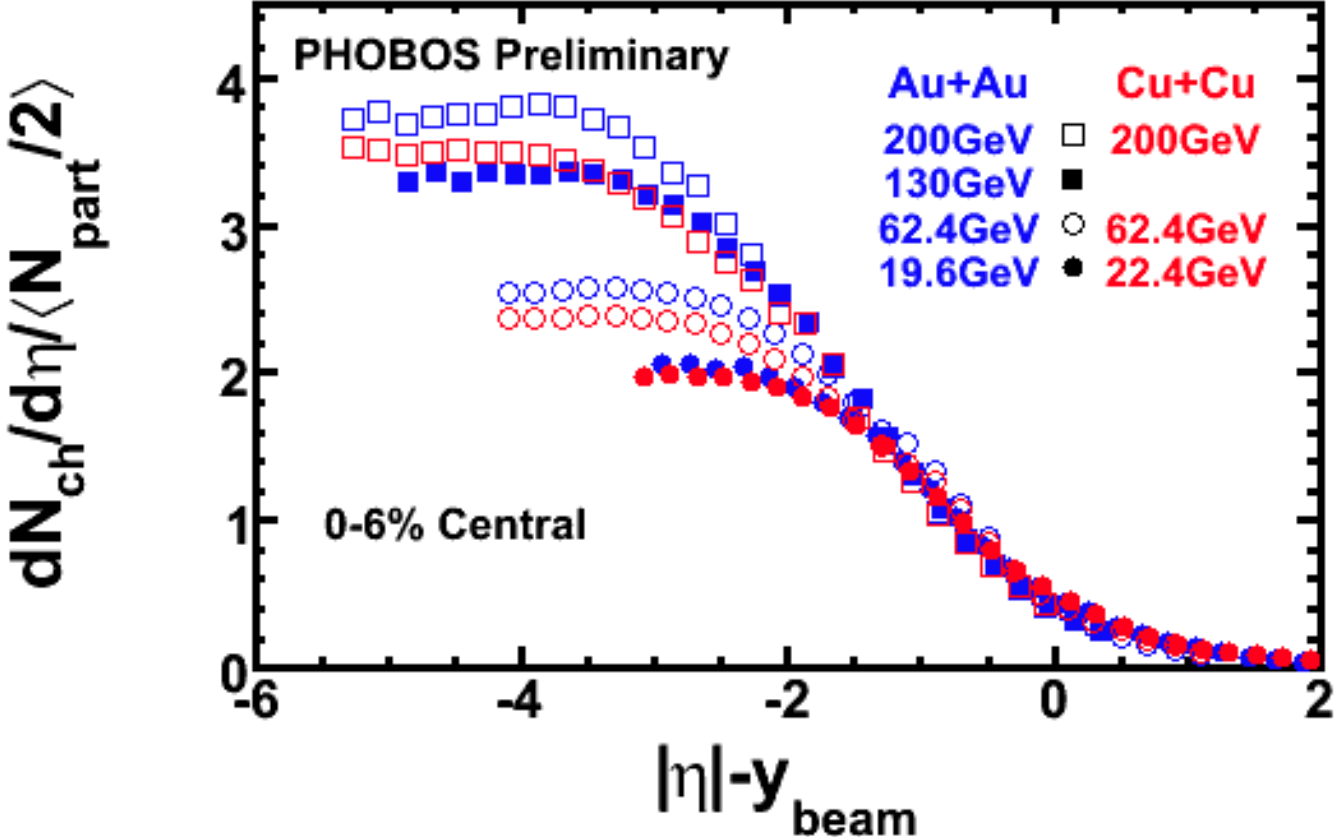
ideal Hydro with CGC vs. Glauber initial conditions



T. Hirano et al., Phys. Lett. B636 (2006) 299

Limiting fragmentation

« Extended longitudinal scaling »



k_T factorization and gluon saturation

k_T factorization for gluon production at high energy $s \gg p_T$:

$$\frac{dN}{dyd^2p_T} = \frac{\alpha_s S_{AB}}{2\pi^4 C_F S_A S_B} \frac{1}{p_T^2} \int \frac{d^2k_T}{(2\pi)^2} \phi_A(x_1, k_T) \phi_B(x_2, |p_T - k_T|)$$

- $S_{A,B}$ total transverse area for nuclei, S_{AB} transverse area for an overlap region.
- p_T transverse momentum of the produced gluon.
- $x_1 = \frac{p_T}{m} e^{y-Y_{\text{beam}}}$, $x_2 = \frac{p_T}{m} e^{-y-Y_{\text{beam}}}$; longitudinal momentum fractions of the gluons probed in target and projectile.
- Functions $\phi(x, k_T)$ are *unintegrated* gluon distributions:

$$xg(x, Q^2) \sim \int^{Q^2} d^2k_T \phi(x, k_T)$$

- Experimentally measure hadrons, need to include the fragmentation from gluons (quarks) to pions.

Scaling in limiting fragmentation

(Stasto)

$$\frac{dN}{dY} \simeq \mathcal{N} x_1 f(x_1) = \mathcal{F}(Y - Y_{beam}), x_1 \gg x_2$$

scaling with $Y - Y_{beam}$ (recall $x_1 \sim \exp(Y - Y_{beam})$).

For comparison with data:

- Need to model $\phi_A(x_1, k_T)$ at large x_1 .
- Since $x_1 f(x_1)$ should obey x_1 scaling

$$x_1 f(x_1) = x_1 f(x_1, Q_s^2) = \int^{Q_s^2} dk^2 \phi_A(x_1, k)$$

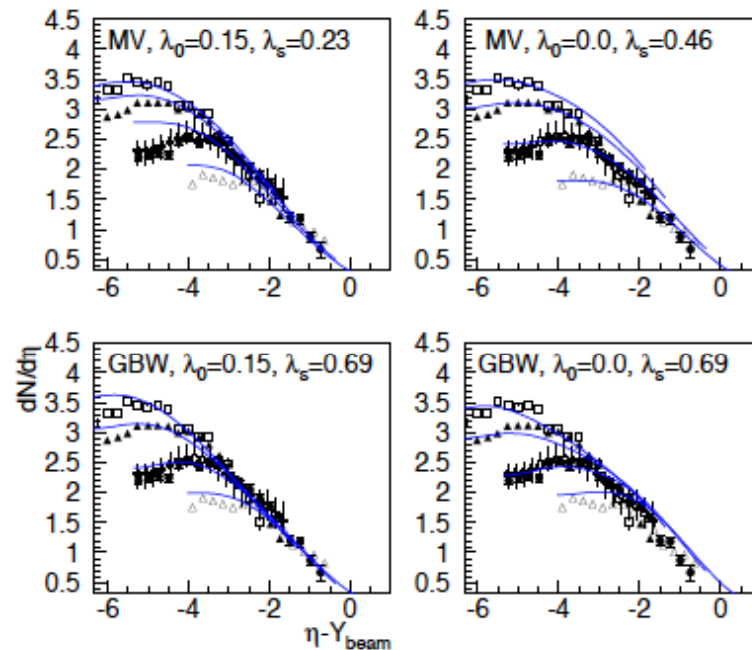
the distribution ϕ_A must be peaked at very low k_T and sharply fall for large k_T .

- $\phi_A(x_1, k_T)$ at large x_1 is the largest source of uncertainty when comparing with the data.

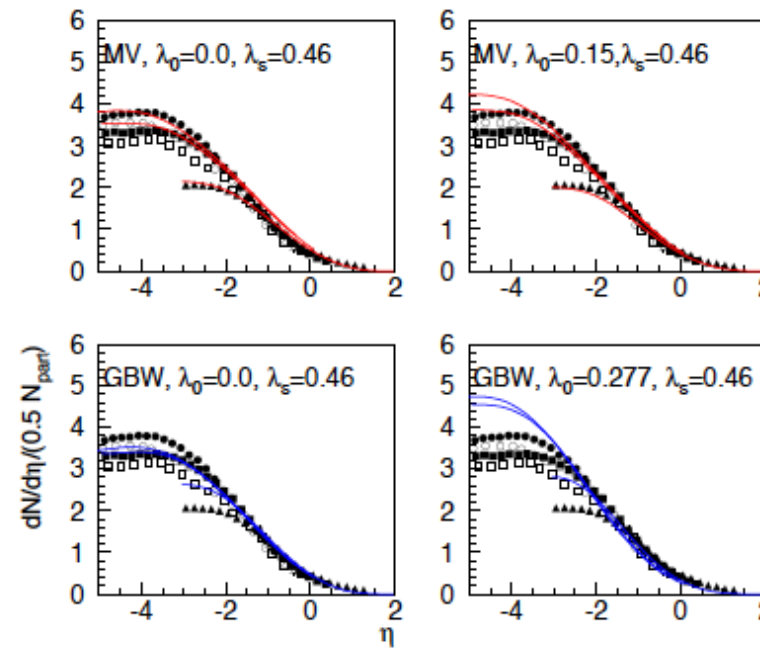
Proton-antiproton and AuAu(central) collisions

Gelis, Venugopalan, A.S.

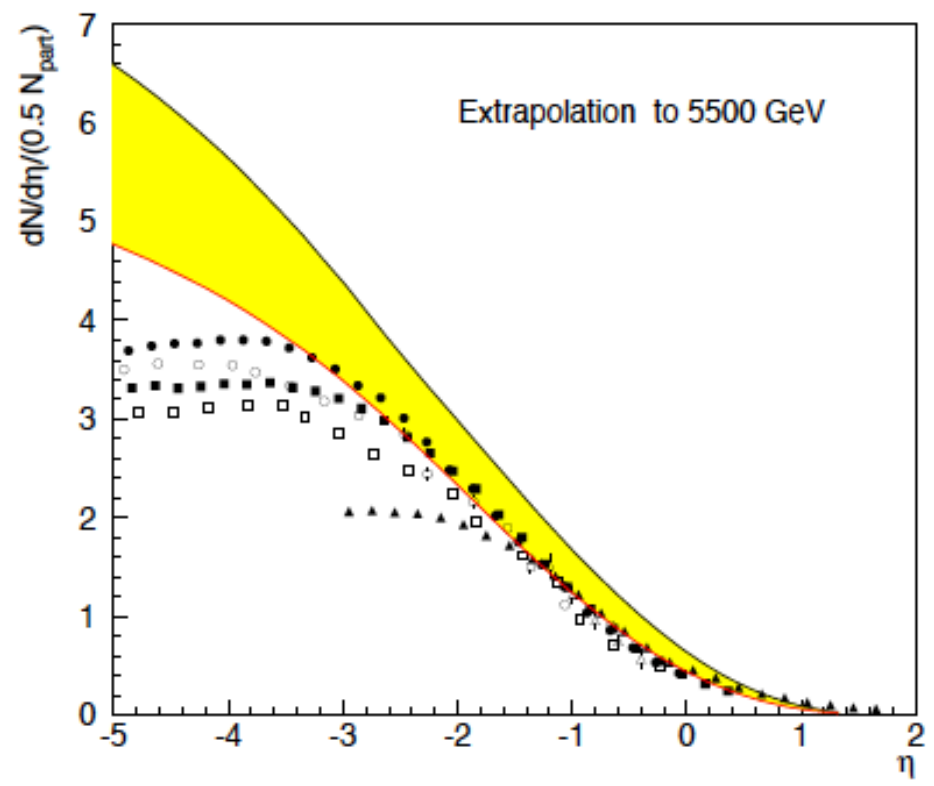
proton-proton:



Gold-Gold central:

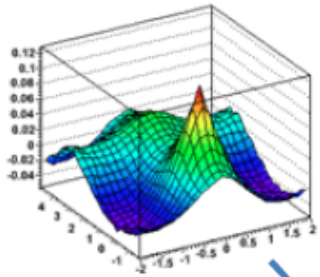


- Small violations of limiting fragmentation scaling due to the fact that in some models we do not have approximately scaling of $x_1 f(x_1)$.
- Additional uncertainties due to $y \leftrightarrow \eta$ change and fragmentation functions.



The Glasma and rapidity correlations

proton-proton

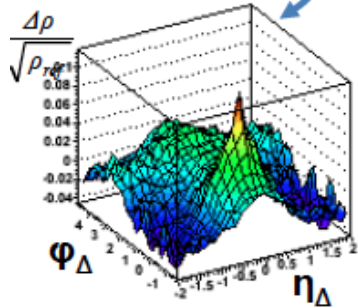


200 GeV Au-Au data

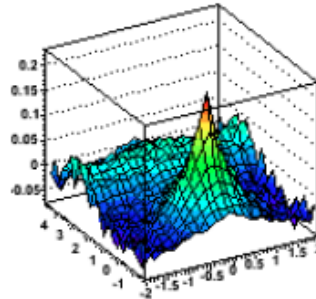
(Ray)

Analyzed 1.2M minbias 200 GeV Au+Au events;
included all tracks with $p_t > 0.15$ GeV/c, $|\eta| < 1$, full ϕ

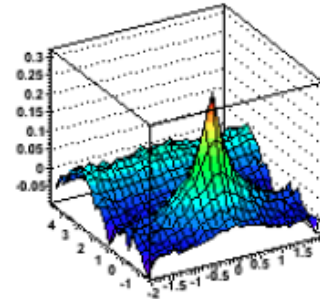
84-93%



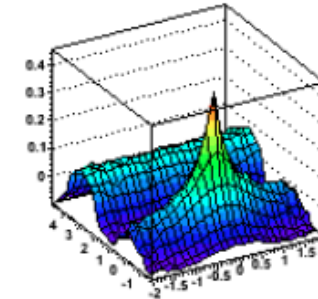
74-84%



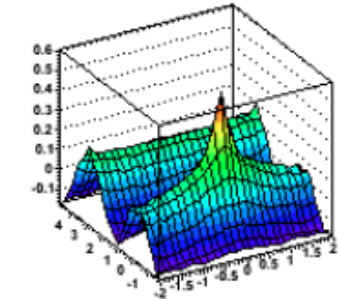
64-74%



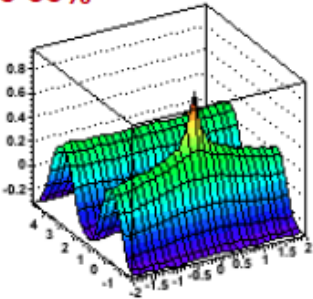
55-64%



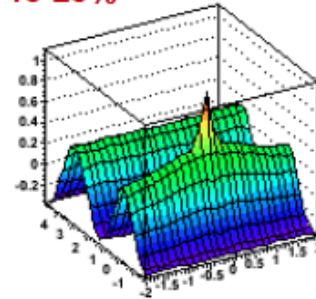
46-55%



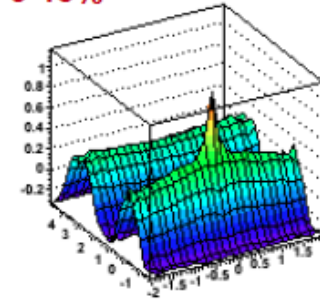
28-38%



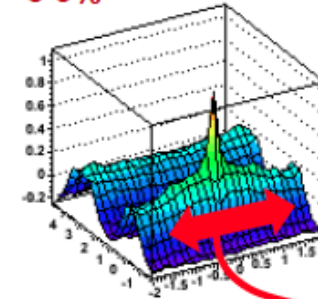
18-28%



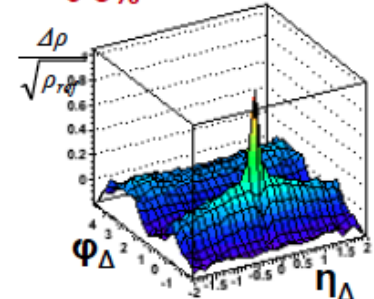
9-18%



5-9%



0-5%



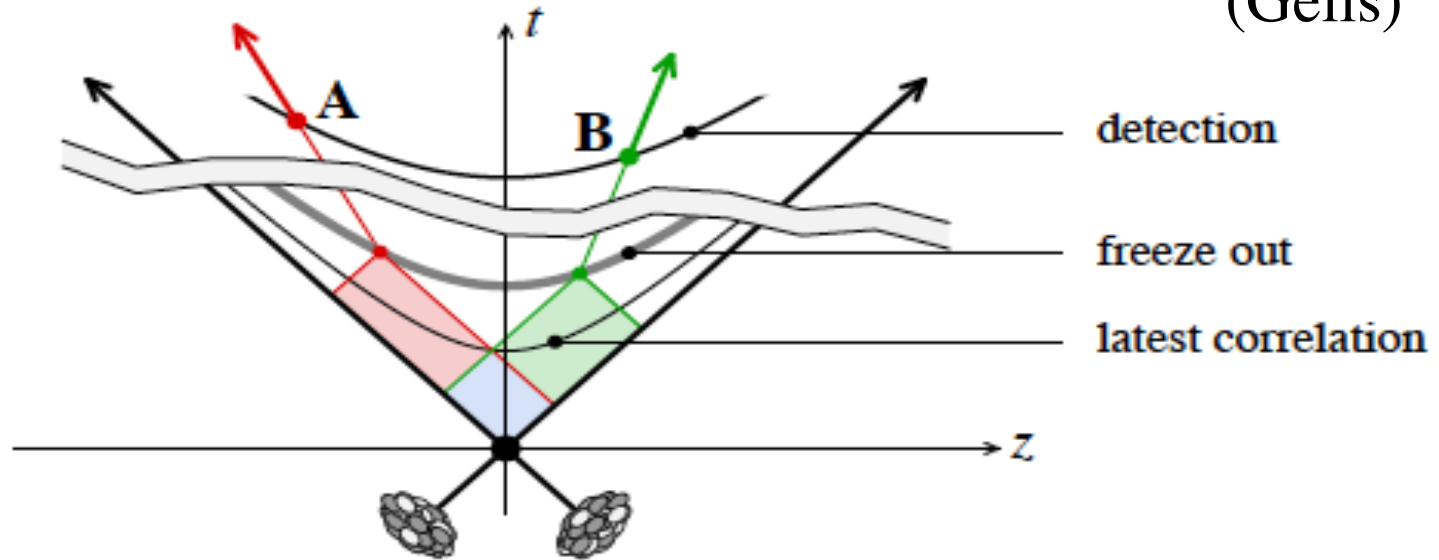
STAR Preliminary

We observe the evolution of several correlation structures including the same-side low p_t ridge

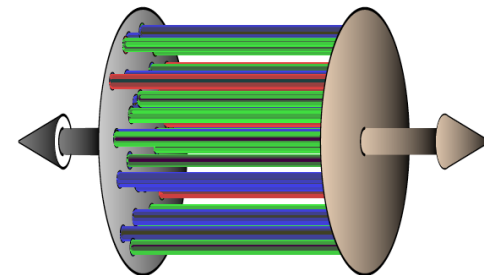
Similar analysis was done for minbias Au-Au at 62 GeV and Cu-Cu at 62 and 200 GeV

Rapidity correlations are established at early times

(Gelis)



The glasma has such correlations
(but other models also - Pajares/Milhano)



Glasma + Blast Wave \Rightarrow Ridge Height

pair correlation function -- Cooper Frye freeze out

$$\Delta\rho \equiv \text{pairs} - (\text{singles})^2 \propto \iint_{\text{freezeout surface}} f(p_1, x_1) f(p_2, x_2) c(x_1, x_2)$$

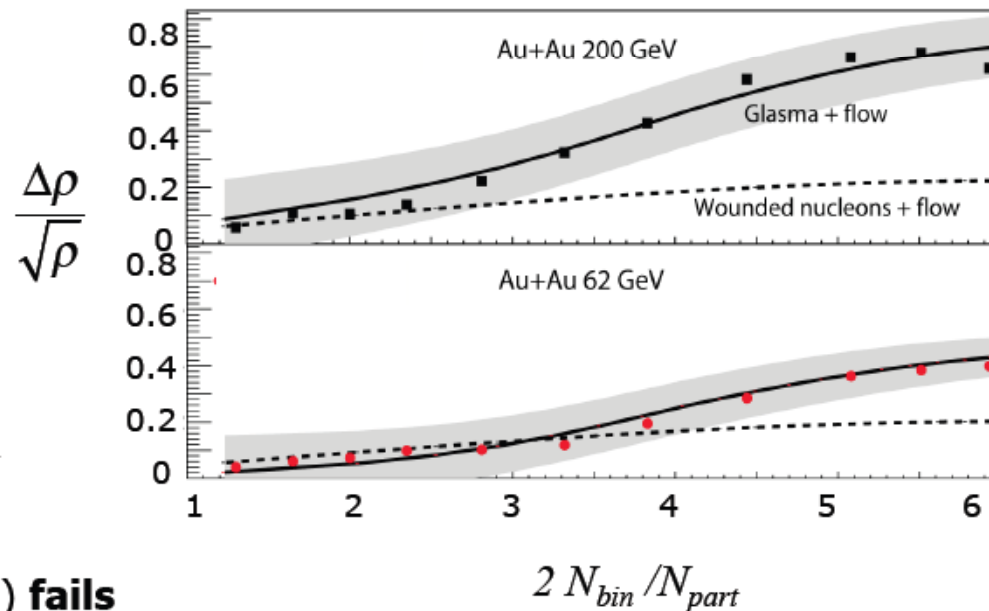
- blast wave $\rightarrow f(p, x)$
- scale factor to fit 200 GeV only
- Glasma energy dependence

$$\mathcal{R} dN/dy \propto \alpha_s^{-1}(Q_s)$$

Glasma Q_s dependence: 200 GeV
Au+Au \Rightarrow 62 GeV, Cu+Cu

wounded nucleon model (dashed) **fails**

STAR Data, J.Phys. G35 (2008) 104090
SG, McLerran, Moschelli et al. PRC 79 (2009) 051902

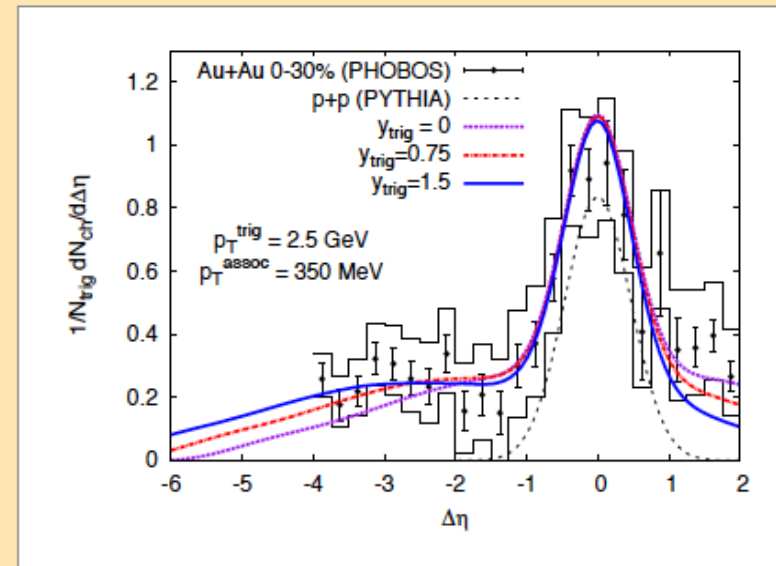
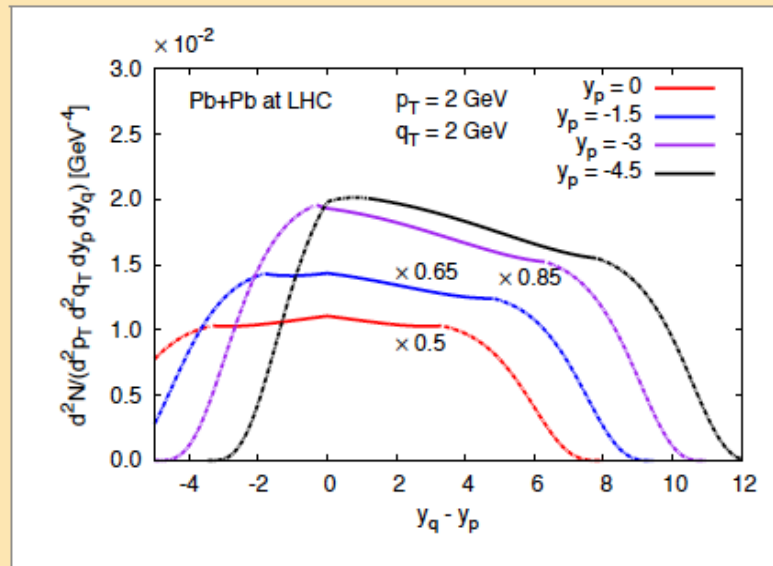


First calculation of rapidity dependence

(Lappi)

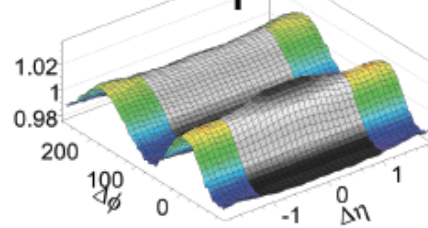
k_T -factorized approximation Dusling, Gelis, T.L., Venugopalan, -09

$$C(\mathbf{p}, \mathbf{q}) \sim \int_{\mathbf{k}_T} \left\{ \overbrace{\Phi_{A_1}^2(y_p, \mathbf{k}_T) \Phi_{A_2}(y_p, \mathbf{p}_T - \mathbf{k}_T)}^{3 \text{ at } y_p} \overbrace{\Phi_{A_2}(y_q, \mathbf{q}_T + \mathbf{k}_T)}^{1 \text{ at } y_q} + (\mathbf{k}_T \leftrightarrow -\mathbf{k}_T) + (A_1 \leftrightarrow A_2) \right\}$$

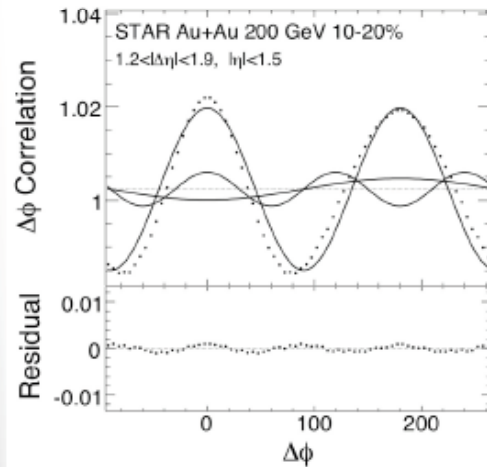


Correlations at large $\Delta\eta$

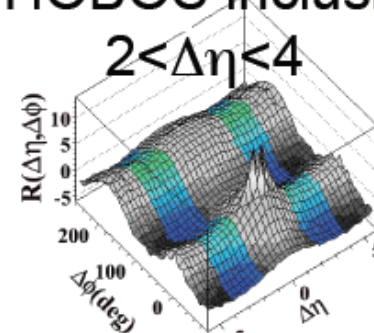
STAR inclusive
 $1.2 < \Delta\eta < 1.9$



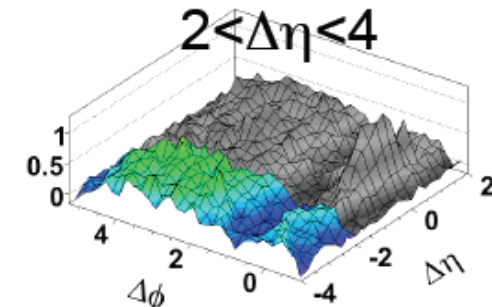
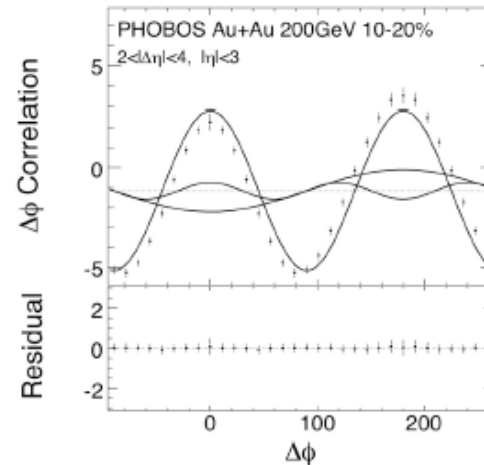
arXiv:0806.0513



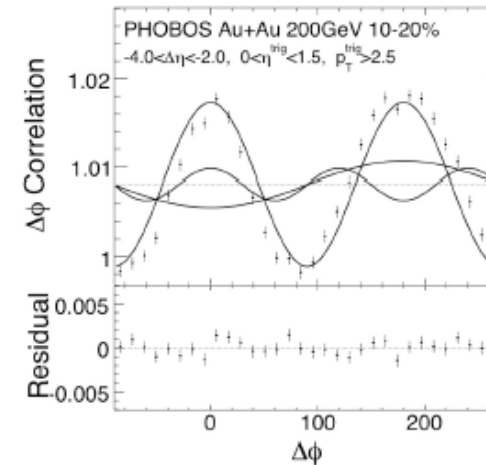
PHOBOS inclusive PHOBOS $p_T^{\text{trig}} > 2\text{GeV}$
 $2 < \Delta\eta < 4$



PRC 81, 024904 (2010)



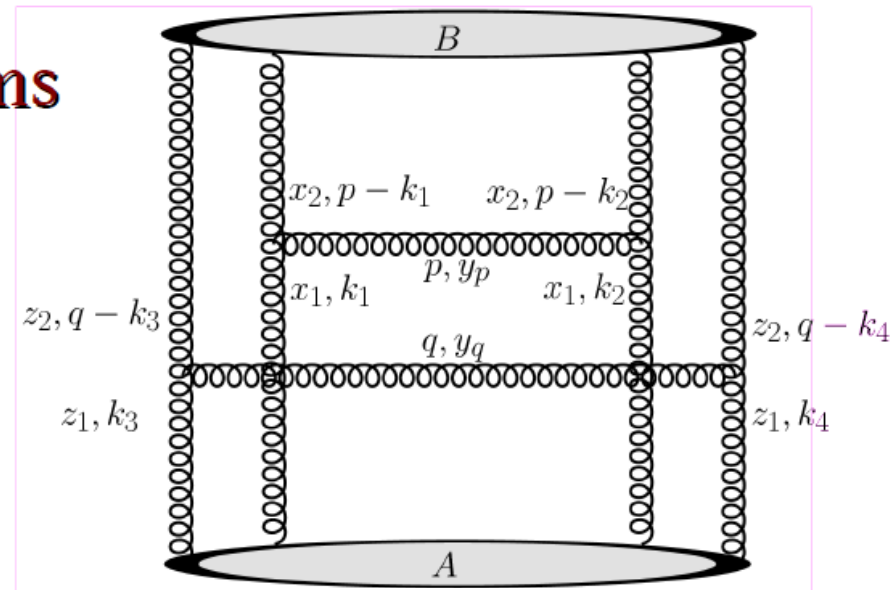
PRL 104, 06230 (2010)



Long range correlations are well described by 3 Fourier Components.

(Dumitru)

**genuine B-JIMWLK terms
from THIS diagram:**



B-JIMWLK four-point function (in Gaussian approximation), incl. “Nc corrections”:

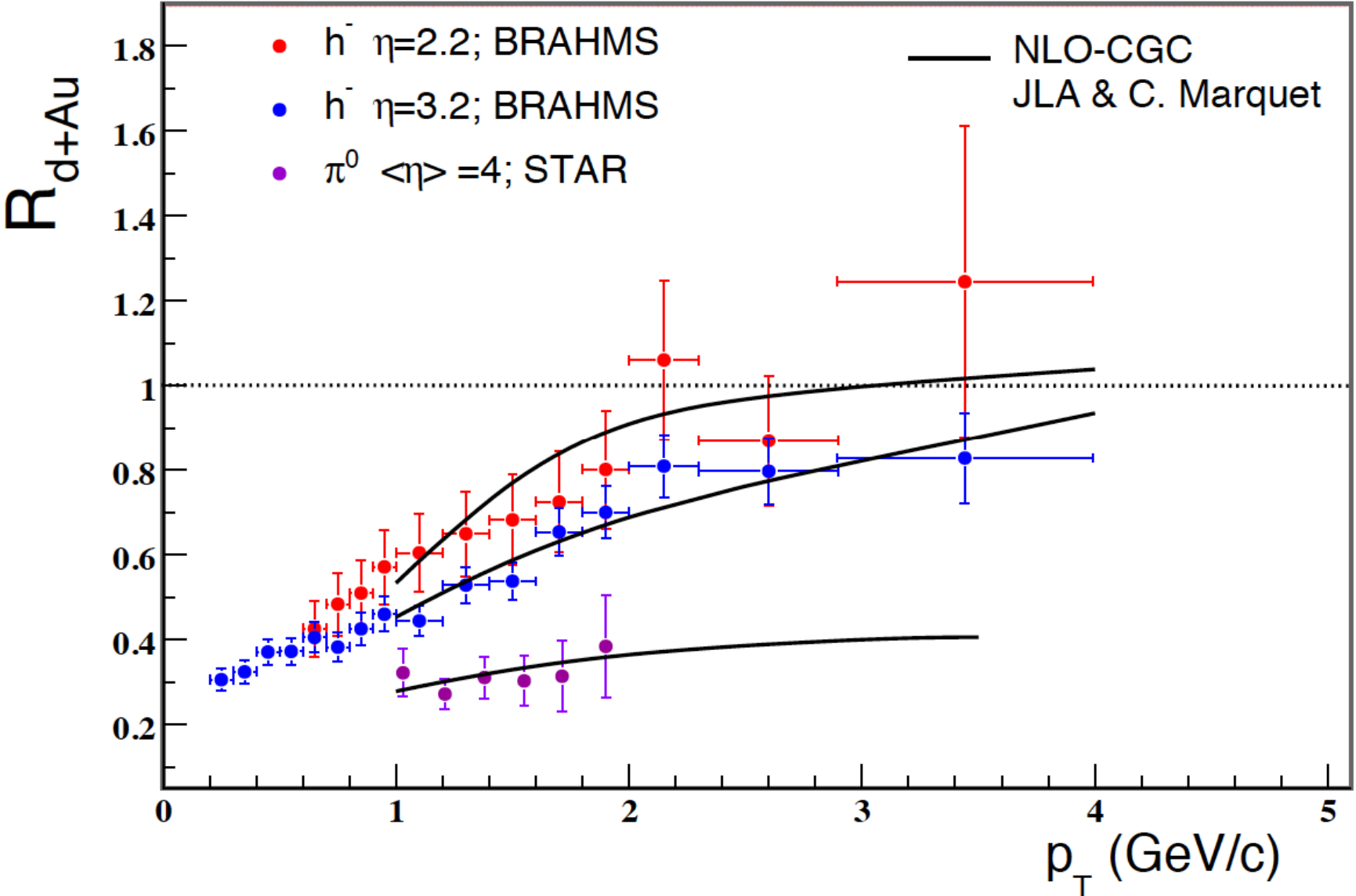
$$\langle \rho^a \rho^b \rho^c \rho^d \rangle = \delta^{ab} \delta^{cd} \langle \rho^2 \rangle^2 + \frac{1}{N_c} f^{abe} f^{cde} \mathcal{F}(k_i) \langle \rho^2 \rangle^2 + \dots$$

A.D., J. Jalilian-Marian,
arXiv:1001.4820

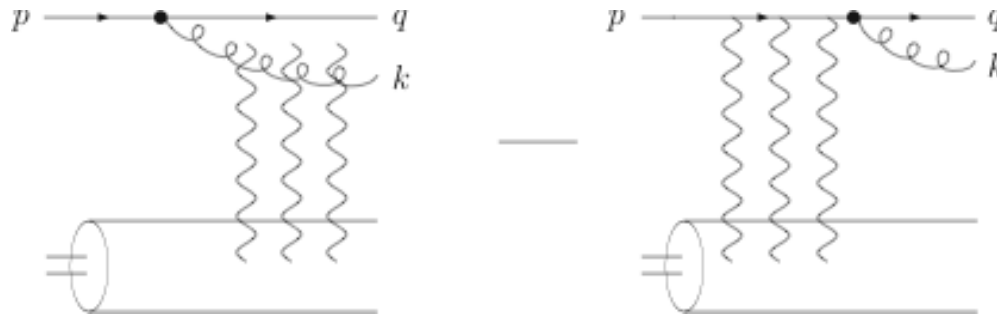
★ ridge in pp @ LHC ?!

Forward rapidity

(Albacete)



Forward di-jet production



collinear factorization of quark density in deuteron

b: quark in the amplitude
x: gluon in the amplitude
b': quark in the conj. amplitude
x': gluon in the conj. amplitude

Fourier transform k_{\perp} and q_{\perp}
 into transverse coordinates

$$\frac{d\sigma^{dAu \rightarrow qqX}}{d^2k_{\perp} dy_k d^2q_{\perp} dy_q} = \alpha_S C_F N_c x_d q(x_d, \mu^2) \int \frac{d^2x}{(2\pi)^2} \frac{d^2x'}{(2\pi)^2} \frac{d^2b}{(2\pi)^2} \frac{d^2b'}{(2\pi)^2} \overbrace{e^{ik_{\perp} \cdot (\mathbf{x}' - \mathbf{x})} e^{iq_{\perp} \cdot (\mathbf{b}' - \mathbf{b})}}$$

$$|\Phi^{q \rightarrow qq}(z, \mathbf{x} - \mathbf{b}, \mathbf{x}' - \mathbf{b}')|^2 \left\{ S_{qq\bar{q}q}^{(4)}[\mathbf{b}, \mathbf{x}, \mathbf{b}', \mathbf{x}'; x_A] - S_{qq\bar{q}}^{(3)}[\mathbf{b}, \mathbf{x}, \mathbf{b}' + z(\mathbf{x}' - \mathbf{b}'); x_A] \right.$$

↓
 pQCD $q \rightarrow qq$
 wavefunction

$$\left. - S_{q\bar{q}q}^{(3)}[\mathbf{b} + z(\mathbf{x} - \mathbf{b}), \mathbf{x}', \mathbf{b}'; x_A] + S_{q\bar{q}}^{(2)}[\mathbf{b} + z(\mathbf{x} - \mathbf{b}), \mathbf{b}' + z(\mathbf{x}' - \mathbf{b}'); x_A] \right\}$$

interaction with hadron 2 / CGC

$$z = \frac{|k_{\perp}| e^{y_k}}{|k_{\perp}| e^{y_k} + |q_{\perp}| e^{y_q}}$$

n-point functions that resums the powers of $g_s A$ and the powers of $\alpha_s \ln(1/x_A)$

computed with JIMWLK evolution at NLO (in the large- N_c limit),

and MV initial conditions

no parameters

Monojets in central d+Au

- in central collisions where Q_s is the biggest

there is a very good agreement of the saturation predictions with STAR data

Albacete and C.M., to appear

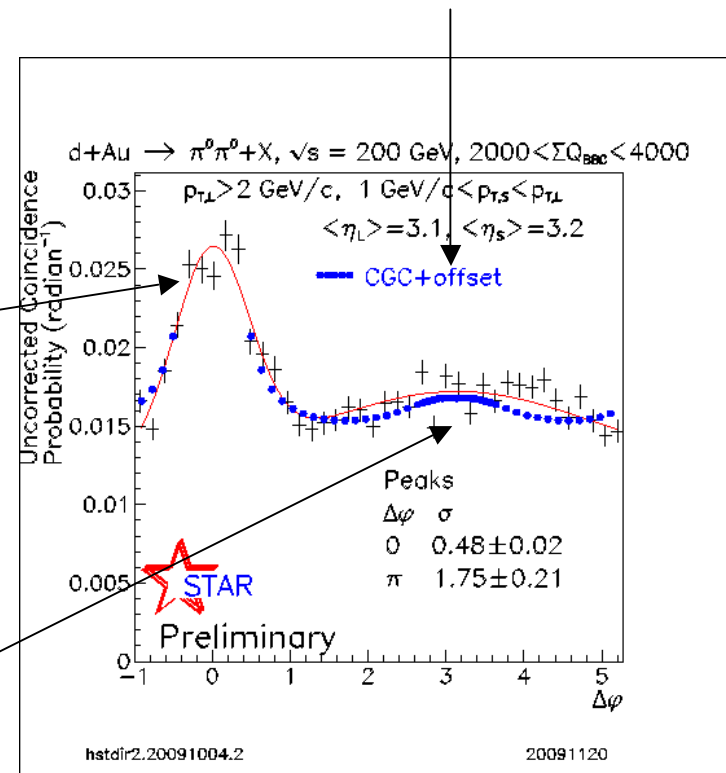
to calculate the near-side peak, one needs di-pion fragmentation functions

- the focus is on the away-side peak

where non-linearities have the biggest effect

suppressed away-side peak

an offset is needed to account for the background



standard (DGLAP-like) QCD calculations cannot reproduce this

(Strikman)

Independent of details - the observed effect is a strong evidence for breaking pQCD approximation in the kinematics sensitive to strong gluon field in nuclei

New forward forward pion data qualitatively consistent with increase of the suppression for this kinematics in $2 \rightarrow 2$ scenario as the second jet is also in BDR. Stronger post selection effect - enhanced effective energy losses.

Relevant effects:

- ➡ second jet is mostly from gluons which have larger effective energy losses
- ➡ x_2 is in the region where gluon shadowing is a factor of 2 - a factor of two smaller relative contribution of forward-forward vs forward inclusive
- ➡ forward-forward events correspond to larger x_1 than forward triggers (next slide) - further enhancement of suppression due to fractional energy losses.

J/Psi

Nuclear effects

3 Initial state saturation of gluons

Due to saturation gluons experience broadening with the coefficient $C(s)$ known from DIS data.

$$\Delta p_T^2 = 2C(s) T_A(b)$$

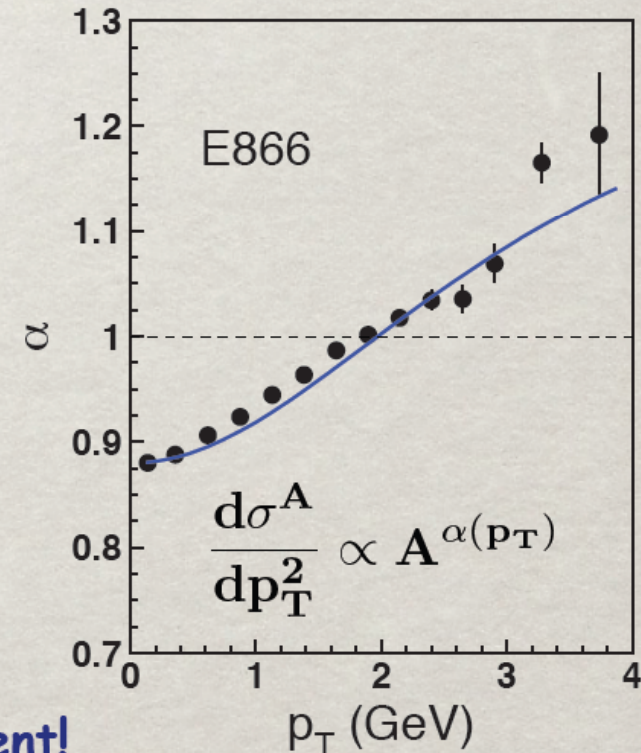
The p_T distribution of J/Ψ has the form:

$$\frac{d\sigma}{dp_T^2} \propto \left(1 + \frac{p_T^2}{6\langle p_T^2 \rangle}\right)^{-6}$$

Broadening results in $\langle p_T^2 \rangle \Rightarrow \langle p_T^2 \rangle + \Delta p_T^2$

$$R_T(p_T) = \frac{\frac{d\sigma}{dp_T^2} \Big|_{\langle p_T^2 \rangle + \Delta p_T^2}}{\frac{d\sigma}{dp_T^2} \Big|_{\langle p_T^2 \rangle}}$$

★ This can be tested with the E866 data for J/Ψ production in pA at 800 GeV:



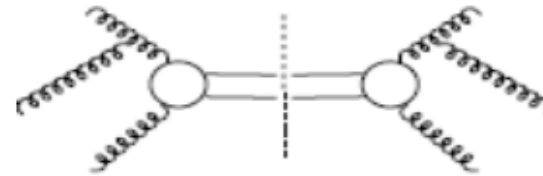
Works amazingly well with no adjustment!

Broadening of heavy quarkonia

Initial-state only:

$$\Delta\langle q_T^2 \rangle_{J/\psi}^{(I)} = C_A \left(\frac{8\pi^2 \alpha_s}{N_c^2 - 1} \lambda^2 A^{1/3} \right)$$

$$\Delta\langle q_T^2 \rangle_{DY} \approx C_F \left(\frac{8\pi^2 \alpha_s}{N_c^2 - 1} \lambda^2 A^{1/3} \right)$$



Kang, Qiu, PRD77(2008)

Experimental data from d+A:

Clear $A^{1/3}$ dependence

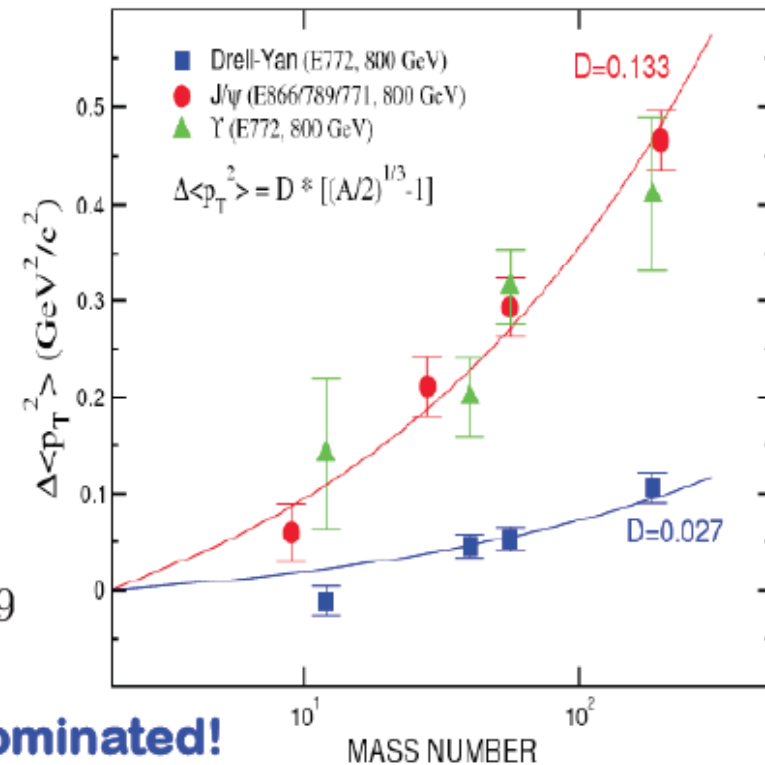
But, wrong normalization!

$$\Delta\langle q_T^2 \rangle_{J/\psi}^{(I)} / \Delta\langle q_T^2 \rangle_{DY} \Big|_{\text{thy}} = C_A / C_F = 2.25$$

$$\Delta\langle q_T^2 \rangle_{J/\psi}^{(I)} / \Delta\langle q_T^2 \rangle_{DY} \Big|_{\text{exp}} = 0.133 / 0.027 \approx 4.9$$

Final-state effect – octet channel dominated!

Only depend on observed quarkonia

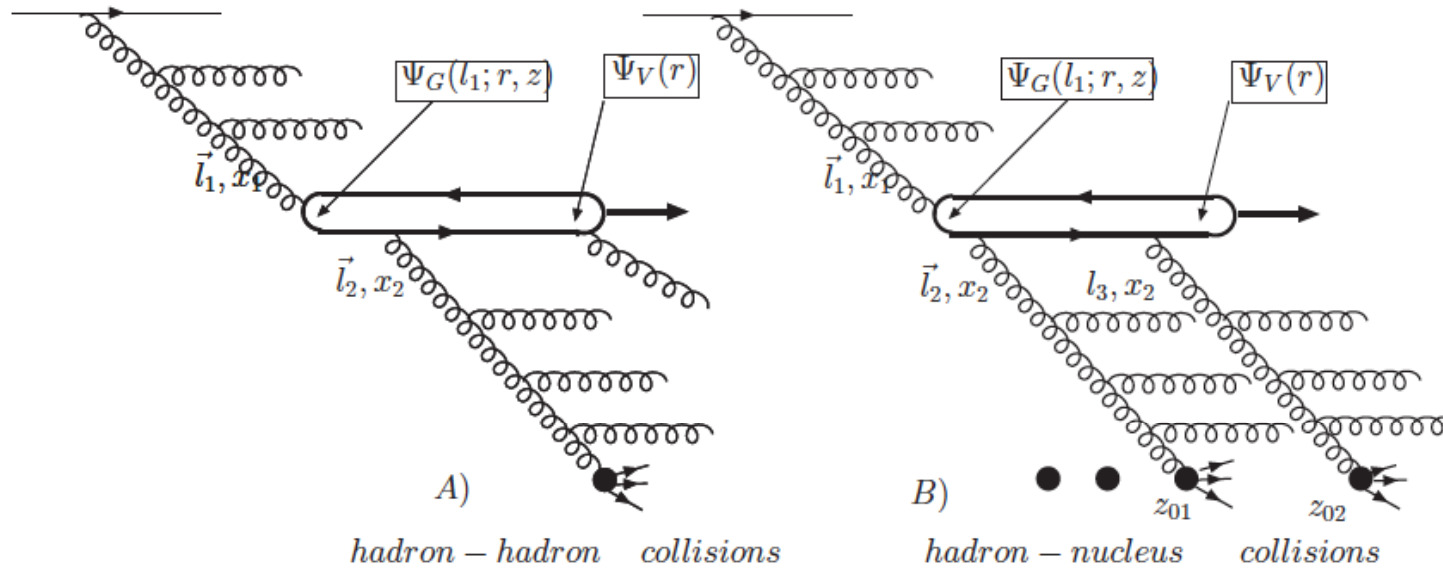


J.C.Peng, hep-ph/9912371

Johnson, et al, 2007

Production of J/ψ : pp vs pA

Kharzeev, KT,2005
Kharzeev, Levin, Nardi, KT,2009



$$\alpha_s^3 A^{1/3} = \alpha_s (\alpha_s^2 A^{1/3}) \sim \alpha_s$$

$$\alpha_s^4 A^{2/3} = (\alpha_s^2 A^{1/3})^2 \sim 1$$

This mechanism is dominant for central collisions

Summary